

Transition in electron transport in a cylindrical Hall thruster

J. B. Parker,^{a)} Y. Raiteses, and N. J. Fisch

Princeton Plasma Physics Laboratory, Princeton University, Princeton, New Jersey 08543, USA

(Received 24 May 2010; accepted 16 August 2010; published online 1 September 2010)

Through the use of high-speed camera and Langmuir probe measurements in a cylindrical Hall thruster, we report the discovery of a rotating spoke of increased plasma density and light emission which correlates with increased electron transport across the magnetic field. As cathode electron emission is increased, a sharp transition occurs where the spoke disappears and electron transport decreases. This suggests that a significant fraction of the electron current might be directed through the spoke. © 2010 American Institute of Physics. [doi:10.1063/1.3486164]

Electron transport in $\mathbf{E} \times \mathbf{B}$ plasma discharges is an interesting topic from both a basic physics and an applied point of view. It is important as a practical matter because electron transport directly affects a device's electrical efficiency. From a basic scientific standpoint, it is interesting because many devices exhibit levels of transport across the magnetic field which cannot be explained by a classical collision mechanism. Instead, anomalous cross-field transport is observed in a myriad of $\mathbf{E} \times \mathbf{B}$ plasma discharges¹ and their applications,² such as magnetrons and Hall thrusters. For Hall thrusters in particular, two commonly proposed anomalous transport mechanisms include Bohm diffusion^{3,4} and near-wall conductivity.⁵

A third possible mechanism for electron transport, the so-called rotating spoke, has also been investigated in an annular geometry with an axial electric field and radial magnetic field, where it was found that the spoke could quantitatively explain the level of anomalous transport.⁶ A qualitative understanding for how the spoke could contribute to electron transport across the magnetic field is as follows: a spoke, or region of increased density, would experience charge separation due to only the electrons being magnetized and undergoing the azimuthal $\mathbf{E} \times \mathbf{B}$ drift. The charge separation generates an E_θ field across the perturbation giving rise to an axial $E_\theta \times \mathbf{B}$ drift for the electrons. In this scenario the spoke's density and electric field fluctuations are in phase, resulting in net electron transport in the direction of the anode.

The cylindrical Hall thruster (CHT) is a promising concept for scaling Hall thruster technology to small size and power.⁷ CHTs have a lower surface-to-volume ratio than conventional annular HTs and may experience less wall erosion. CHTs have operated at powers of 50–300 W and exhibited performance comparable to that of annular HTs.⁸ Interesting discharge phenomena linked to high performance have been observed by increasing the level of cathode electron emission.^{9–11}

In this paper, we describe a rotating spoke of increased light emission and plasma density in a CHT using measurements from a high-speed camera and Langmuir probes. The observed spoke is correlated with higher levels of electron cross-field transport; additionally, as the cathode electron emission is increased, the spoke disappears and electron transport decreases. A connection between increased cathode

electron emission and reduced transport has previously been reported^{11,12} but the discovery of spoke and no-spoke regimes provides a possible underlying explanation.

The CHT used in this work (Fig. 1) has a 2.6 cm channel diameter and a 2.3 cm channel length. The xenon propellant flows through the anode at a rate of 4 SCCM (SCCM denotes cubic centimeter per minute at STP). A discharge voltage of 250 V is applied between the anode and cathode, with typical discharge currents in the range $I_d \sim 0.5$ – 0.7 A. Details of the design and operation have been described elsewhere.¹³ Plasma density n is typically $\sim 3 \times 10^{11}$ cm⁻³ and electron temperature T_e is typically 15 eV.¹⁴ The magnetic profile, which is generated by a current of -2 A in the front electromagnet coil and $+2.5$ A in the back electromagnet coil, features a magnetic cusp near the channel exit. A commercial HeatWave hollow cathode neutralizer serves as the cathode in all data presented here unless otherwise specified. The level of electron emission from the hollow cathode, which is important because it strongly affects thruster operation, can be enhanced with an auxiliary keeper discharge by increasing the keeper current I_k .^{9,11} To check that the observed spoke is intrinsic to the thruster and not induced somehow by the hollow cathode, a simpler wire filament cathode was tested in place of the hollow cathode. The filament cathode has been previously used to operate the CHT and has shown behavior comparable to that of the hollow cathode.¹⁰ The level of electron emission from the wire filament can be con-

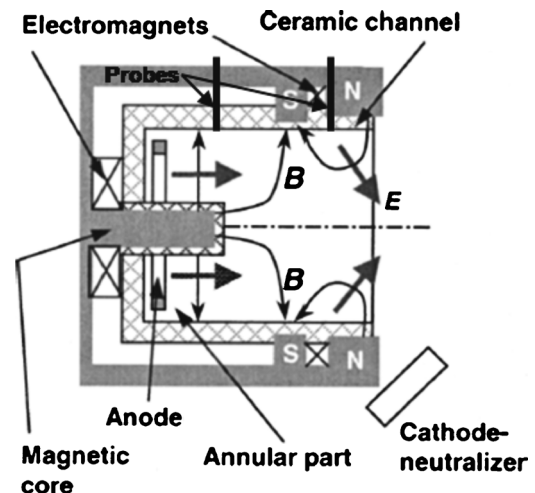


FIG. 1. Schematic of CHT.

^{a)}Electronic mail: jbparker@pppl.gov.

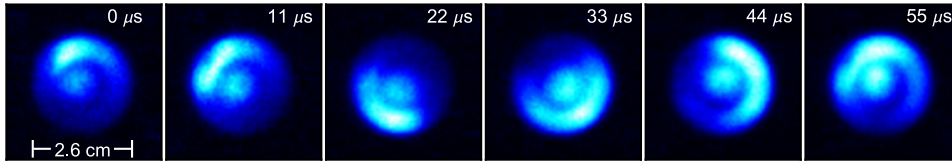


FIG. 2. (Color online) Sequence of camera images (color added) showing a spoke of increased light emission propagating in the $\mathbf{E} \times \mathbf{B}$ direction.

trolled by the amount of heating applied to the wire.¹⁰ Note that increasing the level of electron emission from the cathode does not necessarily increase the current from the cathode. The additional electrons, through a complicated interaction with the thruster and plume plasma, affect the electric field profile in such a way as to limit the current to an equilibrium value.

A discussion of the Langmuir probes used in the CHT can be found elsewhere.¹⁴ Planar probes separated by 90° azimuthally are placed with two probes located at 5 mm and two probes located at 17.5 mm from the anode (Fig. 1). These probes, which are placed such that the collecting surface of the wire is flush with the channel wall, are biased in the ion saturation regime. In order to compare the magnitude of probe signals from different axial locations, each probe should be biased to the same value of $V_p - V_{pl}(z)$, where V_p is the probe bias potential and V_{pl} is the plasma potential. In practice, we hold $V_p - V_f(z)$ constant and equal to -40 V, where the local floating potential V_f is measured with a multimeter. Batteries are used to bias the probes to minimize circuit noise. Ion saturation current fluctuations are measured using 1 kΩ current shunts and a digital oscilloscope at a sample rate of 1 MHz. An additional probe in the plume is used for measurement of ion current I_i ,¹¹ which allows for a calculation of current utilization $\eta_c = I_i/I_d$. The inverse current utilization parameter η_c^{-1} characterizes the level of cross-field electron transport.

A Phantom Camera V7.3 captures unfiltered emissions in the visible spectrum. The camera records at 90 000 frames per second with a 64 × 64 pixel resolution. It is located outside the vacuum vessel looking in through a viewport that is ~ 7 m away from the channel exit along the thruster axis.

Using the camera, we observe the rotating spoke as a region of increased visible light emission that propagates azimuthally. The spoke is seen only in the magnetic “cusp” configuration and is not seen in the “direct” configuration. A sequence of images from the high speed camera is shown in Fig. 2. The spoke travels in the $\mathbf{E} \times \mathbf{B}$ direction with a speed that ranges from $\sim 1.2\text{--}2.8 \times 10^3$ m/s (15–35 kHz). It reverses direction when the magnetic fields are reversed (not shown). The spoke speed is not, however, consistent with the azimuthal $\mathbf{E} \times \mathbf{B}$ speed. The minimum E/B speed can be estimated using values¹⁴ of the electric field near the anode to be ~ 30 V/cm and the magnetic field to be ~ 900 G. This yields an E/B speed of $\sim 3 \times 10^4$ m/s, which is about an order of magnitude higher than the spoke speed, so the $\mathbf{E} \times \mathbf{B}$ drift alone cannot explain the spoke motion.

It is difficult to obtain quantitative, local measurements from the camera because the light emission from the xenon is a complicated function of the electron distribution function and furthermore the emission is integrated axially. For local fluctuation measurements, the Langmuir probes inside the channel are used. The probes are biased in the ion saturation regime and it is assumed that fluctuations in the current correspond to plasma density fluctuations. One must be careful of probe disturbance of the oscillation¹⁵ but no qualitative

changes are observed after placing the probes in the thruster and biasing them. The density fluctuations measured by the probes have amplitude $\delta n/n$ of order unity. To analyze these fluctuations in detail, the local wavenumber-frequency spectrum $S(k_\theta, \omega)$ is calculated from simultaneous measurements from two probes.¹⁶ The spectrum $S(k_\theta, \omega)$ is shown for the two axial locations of 5 mm [Fig. 3(a)] and 17.5 mm [Fig. 3(b)] from the anode. The probe spectrum confirms the existence of 15–35 kHz oscillations inside the channel. The oscillation is stronger near the anode. The dominant observed azimuthal wavenumber is close to $k_\theta = +1/r = 0.77$ cm⁻¹. This corresponds to an $m=1$ mode propagating in the $\mathbf{E} \times \mathbf{B}$ direction, which is roughly consistent with visual observation (Fig. 2). When the density fluctuations measured by probes near the anode and the light emission measured by the camera are compared, the maxima in the density correlate well with the maxima in the light emission around the probe, indicating that the same phenomenon is being observed.

For the preceding data, a hollow cathode keeper current I_k of 1.5 A was used which suppresses the 10 kHz breathing mode¹¹ for cleaner probe signals. When I_k is increased, the spoke and other features of the discharge change dramatically once a threshold level is reached. For one typical experiment, the rotating spoke disappears when $I_k > 2$ A. Additionally, when I_k is increased from 2 to 2.5 A, η_c^{-1} drops from 2.1 to 1.6 [Fig. 4(a)], a change due to the decrease in I_d while I_i stays constant. Furthermore, oscillations with frequencies in the megahertz range are excited in the discharge current [Fig. 4(c)]. The camera shows a roughly uniform discharge because any azimuthal structure is averaged out due to oscillations occurring much faster than the camera speed. For this case, the probe data shows no low frequency mode in $S(k_\theta, \omega)$. The threshold keeper current for these effects ranges from 1.6 to 2.2 A in different experiments which is explained by changes in cathode operation due to cathode aging.

In order to verify that the spoke behavior is inherent to the thruster and not caused by the hollow cathode, a filament

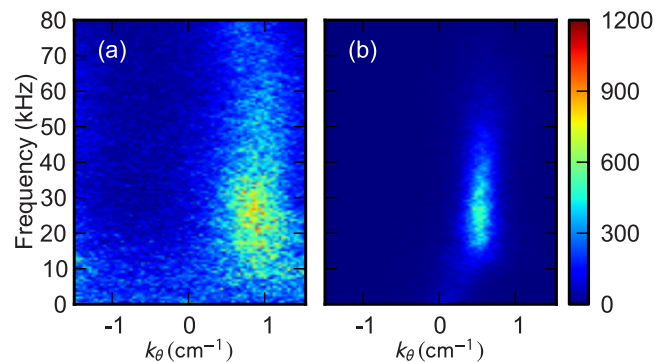


FIG. 3. (Color online) The frequency-wavenumber spectrum $S(k_\theta, \omega)$ is measured using two azimuthal probes separated by 90°. (a) 5 mm from the anode. (b) 17.5 mm from the anode.

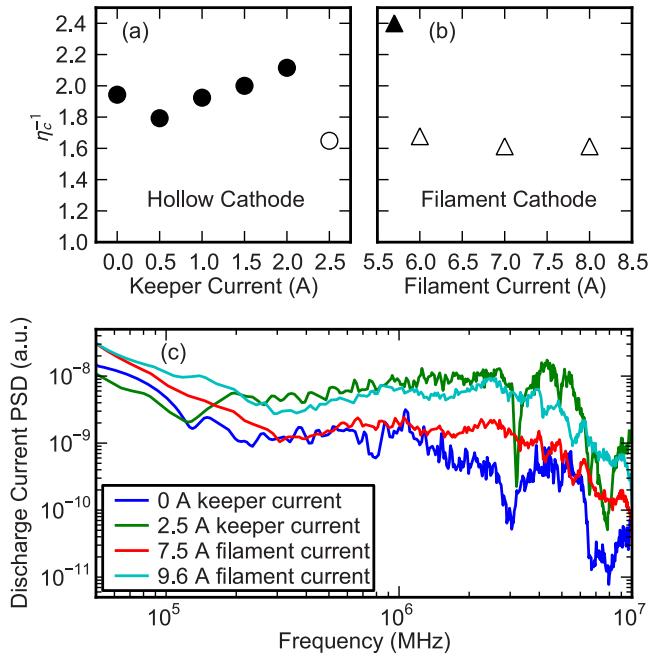


FIG. 4. (Color online) (a) At a threshold in the keeper current of the hollow cathode, η_c^{-1} drops sharply. The spoke is visible for $I_k \leq 2$ A (filled circles), and is not visible at $I_k = 2.5$ A (open circle). The reduced η_c^{-1} at $I_k = 0.5$ A corresponds with a somewhat less coherent spoke, indicating nonmonotonic behavior of the discharge with increasing keeper current. Results shown are typical. (b) Using a filament cathode, η_c^{-1} drops sharply at a threshold in the filament current. The spoke is visible at $I_f = 5.7$ A (filled triangle), and is not visible for $I_f \geq 6$ A (open triangles). Results shown are typical. (c) Power spectral density of the discharge current. High frequency oscillations of order ~ 1 MHz are excited at high keeper current when the hollow cathode is used and high filament current when the filament cathode is used. In this separate experiment, the spoke is visible at $I_f = 7.5$ A and is not visible at $I_f = 9.6$ A; the difference in threshold is due to variations in filament and filament location.

cathode is also tested. With a filament heating current of 5.7 A, a spoke is observed on camera and $\eta_c^{-1} = 2$. When the filament current is increased to 6 A and above, the spoke disappears, η_c^{-1} decreases to 1.7 [Fig. 4(b)] which is mostly due to a decrease in I_d , and oscillations in the megahertz range are excited in the discharge current [Fig. 4(c)].

Because the spoke is observed for both the hollow cathode and the filament cathode, we conclude that the spoke is not strongly dependent on the nature of the cathode. The disappearance of the spoke at increased electron emission is likewise independent of which cathode is used; the corresponding decrease in η_c^{-1} suggests that the spoke may be a major contributor to cross-field electron transport. The high frequency oscillations that are excited when the keeper current or filament current is increased may contribute to the

spoke's disappearance by preventing any coherent structure from forming. It should be noted that in this regime, transport, though reduced, is still higher than expected classically.

For detailed comparison of electron transport levels, one often calculates the Hall parameter $\omega_{ce}\tau$ by assuming that the electron current density is uniform over the cross section A ,^{3,4,8} so that

$$\frac{1}{\omega_{ce}\tau} = \frac{B_r J_{ez}}{E_z en} \sim \frac{B_r I_d - I_i}{enE_z A}. \quad (1)$$

However, given a nonuniform electron current distribution, such as one that may exist in the presence of the spoke, it is not appropriate to use Eq. (1) across different parameter regimes without taking into account the effective cross sectional area. Indeed, the disappearance of the spoke may constitute a large change in effective area. Using Eq. (1) amounts to calculating the cross section-averaged Hall parameter, which conceals any nonuniform physics.

In summary, a rotating spoke has been observed and correlated with electron transport phenomena in a CHT. It is therefore possible that the spoke physics are responsible for the transport, in which case a better understanding of the spoke might enable better control of electron transport.

The authors thank Evan Davis and C. Leland Ellison for contributions to the experiments and Artem Smirnov for fruitful discussions. This material is based upon work supported under an NSF Graduate Research Fellowship. This work was also supported by the U.S. DOE under Contract No. AC02-76CH0-3073 and the AFOSR.

¹J. E. Maggs, T. A. Carter, and R. J. Taylor, *Phys. Plasmas* **14**, 052507 (2007).

²M. Keidar and I. Beilis, *IEEE Trans. Plasma Sci.* **34**, 804 (2006).

³J. P. Boeuf and L. Garrigues, *J. Appl. Phys.* **84**, 3541 (1998).

⁴N. B. Meezan, W. A. Hargus, and M. A. Cappelli, *Phys. Rev. E* **63**, 026410 (2001).

⁵A. I. Morozov and V. V. Savel'ev, in *Reviews of Plasma Physics*, edited by B. B. Kadomtsev and V. D. Shafranov (Springer, New York, 2000), Vol. 21, p. 203.

⁶G. S. Janes and R. S. Lowder, *Phys. Fluids* **9**, 1115 (1966).

⁷Y. Raitses and N. J. Fisch, *Phys. Plasmas* **8**, 2579 (2001).

⁸A. Smirnov, Y. Raitses, and N. J. Fisch, *Phys. Plasmas* **14**, 057106 (2007).

⁹Y. Raitses, A. Smirnov, and N. J. Fisch, *Appl. Phys. Lett.* **90**, 221502 (2007).

¹⁰E. M. Granstedt, Y. Raitses, and N. J. Fisch, *J. Appl. Phys.* **104**, 103302 (2008).

¹¹Y. Raitses, A. Smirnov, and N. J. Fisch, *Phys. Plasmas* **16**, 057106 (2009).

¹²A. Smirnov, Y. Raitses, and N. J. Fisch, *IEEE Trans. Plasma Sci.* **36**, 1998 (2008).

¹³A. Smirnov, Y. Raitses, and N. J. Fisch, *J. Appl. Phys.* **92**, 5673 (2002).

¹⁴A. Smirnov, Y. Raitses, and N. J. Fisch, *J. Appl. Phys.* **95**, 2283 (2004).

¹⁵T. Ito and M. A. Cappelli, *Appl. Phys. Lett.* **94**, 211501 (2009).

¹⁶J. M. Beall, Y. C. Kim, and E. J. Powers, *J. Appl. Phys.* **53**, 3933 (1982).